parameters specified in Table S-1 (see supplementary material). A Z value of 8 requires the presence of two independent molecules per asymmetric unit, and a direct-methods solution revealed the positions of the four unique rhodium atoms. The structure was expanded using the DIRDIF program supplied by the Molecular Structure Corp., whose programs were used for further refinement of the structure. Full-matrix least-squares isotropic refinement of the non-hydrogen atoms was followed by a differential absorption correction using the program DIFABS, after which anisotropic refinement of the Rh and P atoms led to convergence. Hydrogen atoms were placed in idealized positions based on peaks found in a difference Fourier map. Data collection on four other crytals was also undertaken, carefully optimizing data collection parameters by analyzing scan profiles, in an effort to obtain an improved structure. While all data sets gave the same solution, the quality of the refinement was no better than that reported here.

Acknowledgment is made to the U.S. Department of Energy, Office of Basic Energy Sciences, Grant No. FG02-86ER13569, and to the Exxon Education Foundation. NMR spectra were recorded on a Bruker AMX-400 upgraded with funds from National Science Foundation Chemical Instrumentation Award No. 8911868.

Supplementary Material Available: Complete lists of data collection parameters, bond lengths and angles, atomic coordinates, thermal parameters, and least-squares planes (20 pages); a table of calculated and observed structure factors (19 pages). Ordering information is given on any current masthead page.

Insertion of Isocyanides into the Zr–C Bond of Ruthenium/Zirconium Dimetalloalkenes. Spectroscopic and Structural Comparisons of the η^2-Iminoacyl Complexes $Cp(PMe_3)_2RuCH{=}CRC(N^tBu)ZrClCp_2$ (R = H vs R = Me) and Kinetics of Isomerization of a Thermodynamically Unstable η^2-Iminoacyl Complex

Frederick R. Lemke,† David J. Szalda,‡ and R. Morris Bullock*

Department of Chemistry, Brookhaven National Laboratory, Upton, New York 11973

Received July 31, 1991

The reaction of $Cp(PMe_3)_2RuCH{=}CHZrClCp_2$ with ^{t}BuNC produces an η^2-iminoacyl complex, $Cp(PMe_3)_2RuCH{=}CHC(N^tBu)ZrClCp_2$. The initially formed isomer of this compound is the "N-outside" isomer (**2Hk**), where the N-donor portion of the η^2-iminoacyl ligand is on the outside position of the three ligation sites of the Cp_2Zr moiety. This kinetic isomer cleanly rearranges to the thermodynamic "N-inside" isomer (**2Ht**). Activation parameters determined for this rearrangement are $\Delta H^\ddagger = 19.9 \pm 0.6$ kcal mol^{-1}, $\Delta S^\ddagger = -3.4 \pm 2.2$ cal K^{-1} mol^{-1}, and $\Delta G^\ddagger(298\ K) = 20.9$ kcal mol^{-1}. Spectroscopic and crystallographic data for **2Ht** indicate a significant contribution from a zwitterionic resonance form that is facilitated by the disparate electronic properties of the electron-rich ruthenium and the electron-deficient zirconium moieties. The reaction of ^{t}BuNC with the analogous methylated dimetalloalkene $Cp(PMe_3)_2RuCH{=}C(CH_3)ZrClCp_2$ gives the η^2-iminoacyl complex $Cp(PMe_3)_2RuCH{=}C(CH_3)C(N^tBu)ZrClCp_2$ (**2Me**). Spectroscopic and crystallographic data for **2Me** indicate that the presence of a single methyl group has a profound influence on the structural and electronic properties of this η^2-iminoacyl complex, compared to **2Ht**. In contrast to **2Ht**, the metals and the organic bridging group in **2Me** are twisted out of planarity in order to avoid an unfavorable interaction of the methyl group and the ^{t}Bu group. Spectroscopic and structural data suggest negligible contribution from the zwitterionic resonance form in this compound, due to steric inhibition of resonance. The reaction of the less sterically demanding isocyanide MeNC with $Cp(PMe_3)_2RuCH{=}C(R)ZrClCp_2$ (R = H, CH_3) gives $Cp(PMe_3)_2RuCH{=}CHC(NMe)ZrClCp_2$ (**3H**) and $Cp(PMe_3)_2RuCH{=}C(CH_3)C(NMe)ZrClCp_2$ (**3Me**). Spectroscopic data for **3H** and **3Me** and structural data for **3Me** indicate a contribution from a zwitterionic resonance form for both of these η^2-iminoacyl complexes. Crystallographic data for **2Ht**: orthorhombic space group *Pnma*, $a = 16.640$ (3) Å, $b = 13.936$ (3) Å, $c = 13.290$ (3), $V = 3082$ (2) Å^3, $Z = 4$. Crystallographic data for **2Me**: monoclinic space group $P2_1/c$, $a = 13.386$ (3) Å, $b = 22.514$ (6) Å, $c = 10.639$ (3), $\beta = 91.89$ (2)°, $V = 3205$ (3) Å^3, $Z = 4$. Crystallographic data for **3Me**: monoclinic space group $P2_1/n$, $a = 13.031$ (3) Å, $b = 14.880$ (4) Å, $c = 15.594$ (3), $\beta = 108.08$ (2)°, $V = 2874$ (2) Å^3, $Z = 4$.

Insertion of small molecules into metal–carbon bonds is a reaction of fundamental importance in organometallic chemistry.[1] The most thoroughly investigated reaction of this type, migratory insertion of CO into a metal–alkyl bond to form a metal acyl[2] complex, is a critical step in several homogeneous catalytic reactions such as hydroformylation. A reaction that is closely related to the migratory insertions of CO is the reaction of metal alkyl

† Present address: Department of Chemistry, Ohio University, Athens, OH 45701-2979.

‡ Research Collaborator at Brookhaven National Laboratory. Permanent address: Department of Natural Sciences, Baruch College, New York, NY 10010.

(1) For reviews of the CO insertion reaction, see: (a) Alexander, J. J. In *The Chemistry of the Metal-Carbon Bond*; Hartley, F. R., Patai, S., Ed.; Wiley: New York, 1985; Vol. 2; pp 339-400. (b) Calderazzo, F. *Angew. Chem., Int. Ed. Engl.* **1977**, *16*, 299-311. (c) Wojcicki, A. *Adv. Organomet. Chem.* **1973**, *11*, 87-145. (d) Kuhlmann, E. J.; Alexander, J. J. *Coord. Chem. Rev.* **1980**, *33*, 195-225.

(2) For a review of η^2-acyl and η^2-iminoacyl complexes, see: Durfee, L. D.; Rothwell, I. P. *Chem. Rev.* **1988**, *88*, 1059-1079.

0276-7333/92/2311-0876$03.00/0

Scheme I

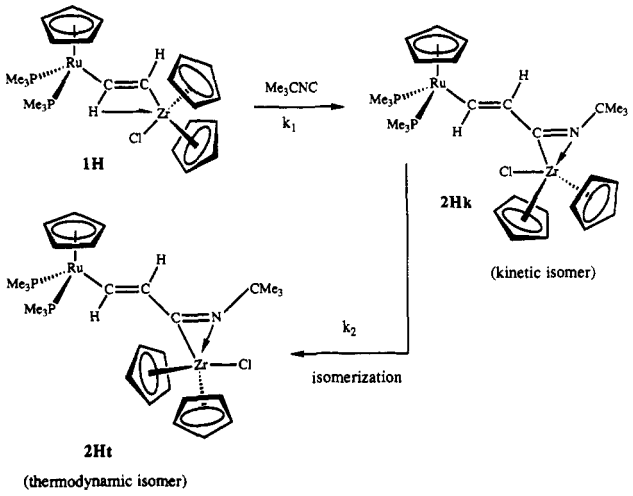

complexes with isocyanides (RN≡C) to form iminoacyl[2] complexes. As in the case of CO insertions, insertions of isocyanides into metal–alkyl bonds are much more commonly observed than insertions into metal–vinyl bonds.

We recently reported the synthesis, spectroscopic properties, and X-ray crystal structures of a series of Ru–Zr complexes

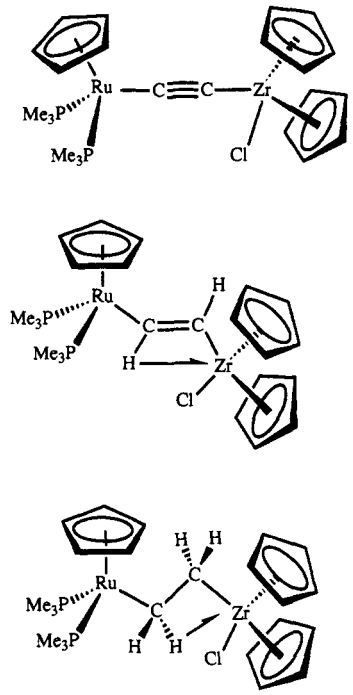

in which C_2 bridges of bond orders 3, 2, and 1 link an electron-deficient Zr moiety to an electron-rich Ru center.[3] In this paper we report synthetic, spectroscopic, and structural studies on the η^2-iminoacyl complexes resulting from reaction of ^{t}BuNC and MeNC with the closely related dimetalloalkene complexes $Cp(PMe_3)_2RuCH{=}C(R)ZrClCp_2$ (R = H, Me). In the case of the reactions with ^{t}BuNC, the presence or absence of the methyl group in the dimetalloalkene has a notable effect on the spectroscopic and structural properties of the products. We also report the kinetics of isomerization of an initially formed iminoacyl complex to its thermodynamic isomer.

(3) (a) Lemke, F. R.; Szalda, D. J.; Bullock, R. M. *J. Am. Chem. Soc.* **1991**, *113*, 8466–8477. (b) Bullock, R. M.; Lemke, F. R.; Szalda, D. J. *J. Am. Chem. Soc.* **1990**, *112*, 3244–3245.

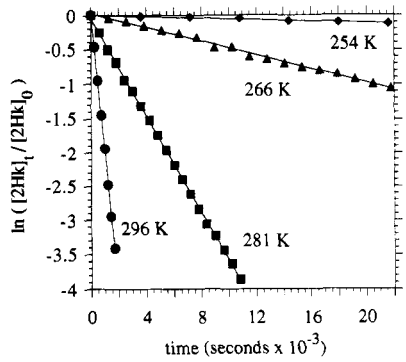

Figure 1. First-order plots for rate of disappearance of **2Hk** at four temperatures. (Only the first six data points collected at 254 K are shown here; the reaction was followed for 22 h, to 40% isomerization, and exhibited a linear first-order plot over this entire range.)

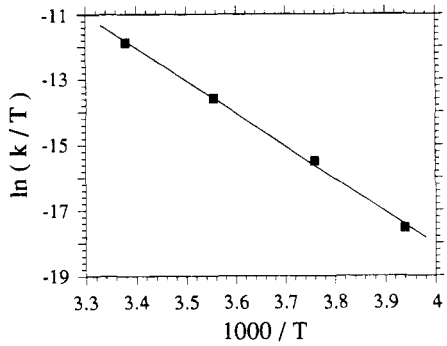

Figure 2. Eyring plot for isomerization of **2Hk** to **2Ht**.

Table I. First-Order Rate Constants for the 2Hk → 2Ht Isomerization

T (K)	k, s^{-1}	T (K)	k, s^{-1}
254	6.17×10^{-6}	281	3.53×10^{-4}
266	4.99×10^{-5}	296	2.05×10^{-3}

Results and Discussion

Formation and Isomerization of an η^2-Iminoacyl Complex. When the reaction of a 0.05 M CD_2Cl_2 solution of $Cp(PMe_3)_2RuCH{=}CHZrClCp_2$ (**1H**) with an eqimolar concentration of ^{t}BuNC was monitored by low-temperature ^{1}H NMR, negligible reaction was observed at 200 K. A slow reaction occurred at 220 K, and after 3 h at 260 K, new resonances had appeared which are assigned to an η^2-iminoacyl complex. This initially formed product is assigned as the "N-outside" kinetic isomer (**2Hk**) shown in Scheme I, where the nitrogen donor portion of the η^2-iminoacyl ligand is on the outside, or lateral, position of the three ligation sites of the Cp_2Zr moiety. The intensities of the resonances of this thermodynamically unstable product decrease with time, and new signals appear in the NMR spectrum due to the isomerized product. This product is the "N-inside" thermodynamic isomer (**2Ht**) in which the nitrogen donor portion of the η^2-iminoacyl ligand is on the inside, or central, position. The kinetics of this isomerization were monitored by ^{1}H NMR at four temperatures between 254 and 296 K. As shown in Figure 1, the isomerization reaction is cleanly first-order, with plots of ln ($[\mathbf{2Hk}]_t/[\mathbf{2Hk}]_0$) being linear for up to 6 half-lives. First-order rate constants for the isomerization are given in Table I, and an Eyring plot is shown in Figure 2. The activation parameters determined from the temperature dependence of the rate constants are $\Delta H^\ddagger$ = 19.9 ± 0.6 kcal mol^{-1}, $\Delta S^\ddagger$ = −3.4 ± 2.2 cal K^{-1} mol^{-1}, and $\Delta G^\ddagger$(298 K) = 20.9 kcal mol^{-1}. The low value of the en-

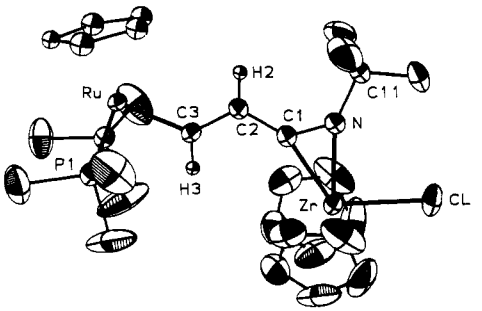

Figure 3. ORTEP drawing of $Cp(PMe_3)_2Ru(CHCHCNCMe_3)$-$ZrClCp_2$ (**2Ht**) with thermal ellipsoids at the 50% probability level. All labeled atoms (except for P(1)) lie on a crystallographic mirror plane. Hydrogen atoms on the methyl groups and those on the cyclopentadienyl ligands are omitted.

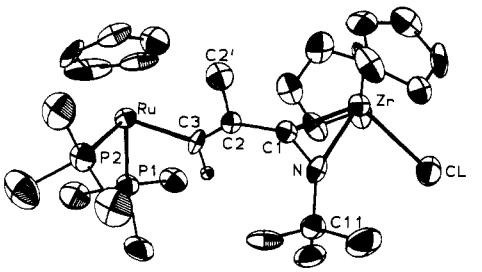

Figure 4. ORTEP drawing of $Cp(PMe_3)_2Ru(CHCMeCNCMe_3)$-$ZrClCp_2$ (**2Me**) with thermal ellipsoids at the 50% probability level. Hydrogen atoms on the methyl groups and those on the cyclopentadienyl ligands are omitted.

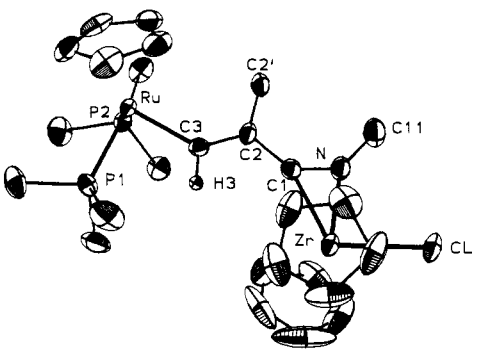

Figure 5. ORTEP drawing of $Cp(PMe_3)_2Ru(CHCMeCNMe)$-$ZrClCp_2$ (**3Me**) with thermal ellipsoids at the 50% probability level. Hydrogen atoms on the methyl groups and those on the cyclopentadienyl ligands are omitted.

tropy of activation is consistent with an intramolecular isomerization.

Erker reported[4] a related isomerization of η^2-acyl complexes in a study of the carbonylation of $Cp_2Zr(CH_3)_2$, Cp_2ZrPh_2, and related complexes. The initially formed "O-outside" isomer of $Cp_2Zr(CH_3)(\eta^2\text{-}COCH_3)$ was spectroscopically observable at low temperature, but it readily rearranges to the "O-inside" η^2-acyl isomer (Scheme II). The acyl isomerizations have much lower activation barriers than the iminoacyl isomerization reported here. For example, $\Delta G^{\ddagger}(150\ K) = 11.4$ kcal mol^{-1} for the "O-outside" → "O-inside" isomerization of $Cp_2Zr(CH_3)(\eta^2\text{-}COCH_3)$. Hoffmann and co-workers have reported[5] calculations on η^2-acyl complexes of zirconocene and actinides. They suggest that the mechanism for the "O-outside" → "O-inside" conversion involves dissociation of the oxygen atom of the η^2-acyl to give an η^1-acyl intermediate, which then rotates and recoordinates to the metal to complete the rearrangement. An analogous η^2-iminoacyl → η^1-iminoacyl (rotation) → η^2-iminoacyl process is suggested to account for the **2Hk** → **2Ht** rearrangement studied here.

Scheme II

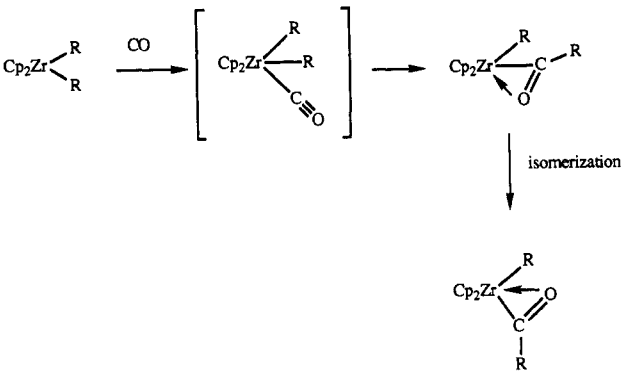

We are not aware of any previous observation of an isomerization of this type for iminoacyl complexes, where a thermodynamically unstable η^2-iminoacyl complex irreversibly rearranges to a stable product. There are, however, examples where fluxional behavior in η^2-iminoacyl complexes has been attributed to a formal rotation of η^2-iminoacyl ligands. Variable-temperature ^{13}C NMR studies by Adams and Chodosh established activation parameters of $\Delta H^{\ddagger} = 14.7 \pm 0.5$ kcal mol^{-1} and $\Delta S^{\ddagger} = -1.7 \pm 1.5$ cal K^{-1} mol^{-1} for the rearrangement of the molybdenum η^2-iminoacyl complex shown in eq 1.[6] Lappert and

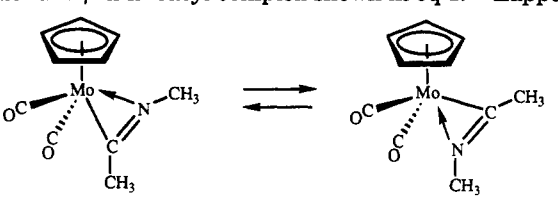

(1)

co-workers[7] found that the two isomers of $Cp_2Zr(Cl)[\eta^2\text{-}(p\text{-tol})NCCH(SiMe_3)_2]$ interconvert (coalescence at 65 °C in C_6D_6 in the ^{13}C NMR). Rothwell and co-workers[8] have observed rotation of the η^2-iminoacyl groups in bis(η^2-iminoacyl)zirconium compounds containing bulky aryloxide ligands, and they reported $\Delta G^{\ddagger}(-40\ °C) = 11.4 \pm 0.5$ kcal mol^{-1} for $(ArO)_2Zr[\eta^2\text{-}(2,6\text{-}Me_2C_6H_4)NCCH_2Ph]_2$ (Ar = 2,6-^{t}Bu$_2$C$_6$H$_3$).

Comparative Rates of Reaction of Isocyanides with the Dimetalloethylene Complex $Cp(PMe_3)_2RuCH$=$CHZrClCp_2$ (1H) and the Dimetallopropylene Complex $Cp(PMe_3)_2RuCH$=$C(CH_3)ZrClCp_2$ (1Me). The dimetallopropylene complex $Cp(PMe_3)_2RuCH$=$C(CH_3)$-$ZrClCp_2$ (**1Me**) also reacts with ^{t}BuNC to produce only one observed η^2-iminoacyl complex, **2Me** (eq 2). Starting material **1Me** differs from **1H** only in having a methyl group rather than H on the carbon bonded to Zr, yet the resulting η^2-iminoacyl products (**2Ht** and **2Me**) differ substantially. The relative rates of reaction of ^{t}BuNC with **1H** and **1Me** were examined in order to determine how the methyl group of the dimetalloalkene affected the kinetics of the insertion reaction. Experiments in separate tubes indicated a dramatic difference in rates of reaction of the

(4) (a) Erker, G. *Acc. Chem. Res.* **1984**, *17*, 103–109. (b) Erker, G.; Rosenfeldt, F. *J. Organomet. Chem.* **1980**, *188*, C1–C4.

(5) (a) Tatsumi, K.; Nakamura, A.; Hofmann, P.; Stauffert, P.; Hoffmann, R. *J. Am. Chem. Soc.* **1985**, *107*, 4440–4451. (b) Hofmann, P.; Stauffert, P.; Tatsumi, K.; Nakamura, A.; Hoffmann, R. *Organometallics* **1985**, *4*, 404–406.

(6) Adams, R. D.; Chodosh, D. F. *Inorg. Chem.* **1978**, *17*, 41–48.

(7) Lappert, M. F.; Luong-Thi, N. T.; Milne, C. R. C. *J. Organomet. Chem.* **1981**, *174*, C35–C37.

(8) Chamberlain, L. R.; Durfee, L. D.; Fanwick, P. E.; Kobriger, L.; Latesky, S. L.; McMullen, A. K.; Rothwell, I. P.; Folting, K.; Huffman, J. C.; Streib, W. E.; Wang, R. *J. Am. Chem. Soc.* **1987**, *109*, 390–402.

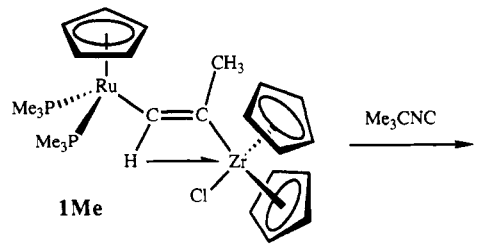

(2)

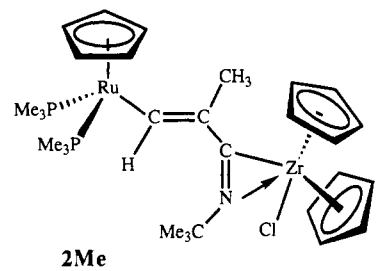

two complexes, with the rate for the methylated compound **1Me** being much slower. The reaction of **1H** with ^{t}BuNC (1 equiv) was ~90% complete in 10 min at 298 K and gave about a 1:1 mixture of the kinetic and thermodynamic isomers, **2Hk** and **2Ht**. After 1.5 h, only the thermodynamic isomer **2Ht** was observed. The analogous reaction of **1Me** with ^{t}BuNC under similar conditions was much slower, giving only ~45% **2Me** after 42 h and being ~72% complete after 6 days. A kinetic isomer of this η^2-iminoacyl complex may be an intermediate in this reaction also, but it was not detected. Along with these qualitative experiments in separate tubes, competition experiments were carried out in which solutions containing both **1H** and **1Me** were allowed to complete for a limited amount of ^{t}BuNC. The results of these experiments indicated a kinetic preference of >100:1 for reaction of ^{t}BuNC with **1H** over **1Me**, in both C_6D_6 and CD_2Cl_2 solution.

The reaction of dimetalloalkenes **1H** and **1Me** with the less sterically demanding isocyanide MeNC produces η^2-iminoacyl complexes **3H** and **3Me** (eq 3). As in the case

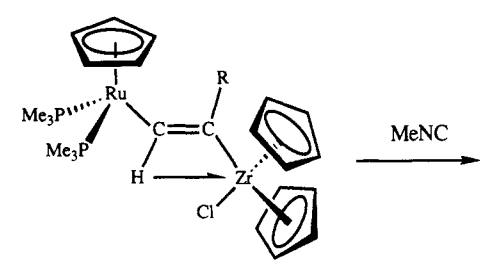

(3)

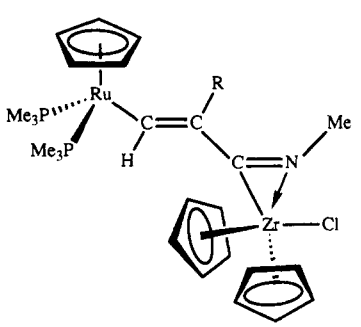

of the reactions with ^{t}BuNC, competition experiments using MeNC revealed a lower limit of >100:1 for the kinetic preference of the reaction of MeNC with **1H** over **1Me**.

Table II. Selected NMR Spectroscopic Data for 2Hk, 2Ht, 2Me, 3H, and 3Me (δ, CD_2Cl_2)

NMR resonance	2Hk	2Ht	2Me	3H	3Me
RuC*H* (^{1}H)	10.49	10.02	6.87	10.09	9.59
RuCH (^{13}C)	222.1	214.2	153.4	216.6	208.7
RuC*C* (^{13}C)	137.2	136.4	141.0	134.8	142.8
*C*N (^{13}C)	204.3	216.5	227.7	218.3	219.4

The dramatic effect of the methyl group on the rate of the reaction of these dimetalloalkenes with isocyanides is apparently caused by the methyl group inhibiting the approach of the isocyanide to the zirconium, since the isocyanide presumably binds to the zirconium prior to the insertion into the Zr–C bond. It is possible that an electronic effect influences the rate of these reactions in addition to the steric effect, since electron donation by the methyl group in **1Me** might help to decrease the electrophilic character of the Zr in **1Me** compared to **1H**. We favor the steric effect over the electronic effect as the predominant factor in determining the rate of these isocyanide insertions. A similar kinetic preference of ~100:1 was observed[3] in the carbonylation of these two dimetalloalkenes to give η^2-acyl complexes.

Isolation and Spectroscopic Characterization of η^2-Iminoacyl Complexes of Dimetalloalkenes. In the NMR experiments described above, the η^2-iminoacyl complexes were synthesized in C_6D_6 or CD_2Cl_2 solution. Preparative reactions were carried out using neat isocyanide as a solvent. Utilization of this unconventional solvent/reagent offers several advantages in the preparation of the η^2-iminoacyl product. Since both ^{t}BuNC and MeNC are volatile, they can be easily manipulated on a vacuum line. When the reaction is complete (usually in less than 1 h), the unreacted excess isocyanide can be recovered by vacuum transfer for future use. An additional advantage is that handling the isocyanides in this way minimizes exposure to these toxic reagents, compared to manipulating them in solution with syringes, etc.

Comparison of the spectroscopic properties of the η^2-iminoacyl complexes reveals significant differences between **2Me** and the other η^2-iminoacyl complexes (Table II). A prominent difference between **2Ht** and **2Me** is in the position of the ^{1}H and ^{13}C NMR resonances of the RuCH moiety. The ^{1}H NMR resonance for RuC*H* is over 3 ppm further downfield in **2Ht** compared to **2Me**, and the difference in ^{13}C NMR resonances of the Ru*C*H moieties in these two compounds is about 60 ppm in the same direction. This and other spectroscopic data, together with the crystallographic data to be discussed later, indicate that the presence of a single methyl group leads to substantial differences in the electronic structures of **2Ht** and **2Me**. In particular, we suggest that **2Ht** has a considerable contribution from the zwitterionic resonance form shown in Scheme III, while **2Me** has a negligible contribution from this resonance structure and is adequately described in terms of the neutral resonance structure depicted in eq 2. The large downfield shifts of the ^{1}H and ^{13}C NMR resonances of RuCH in **2Ht** compared to **2Me** support the existence of the Ru=C carbene character in **2Ht**. Note that the carbon that is β to Ru in the η^2-iminoacyl complexes (i.e., the one that was bonded to Zr in the dimetalloalkene starting material) has similar chemical shifts in the ^{13}C NMR spectrum of **2Ht** and **2Me**, despite the fact that it is this carbon that has a hydrogen bonded to it in **2Ht** but a methyl group bonded to it in **2Me**. This is apparently due to the fact that its bonding is similar in

Table III. Crystallographic Data from the X-ray Diffraction Study of 2Ht, 2Me, and 3Me

	2Ht	2Me	3Me
formula	$C_{28}H_{44}ClNP_2RuZr$	$C_{29}H_{46}ClNP_2RuZr$	$C_{26}H_{40}ClNP_2RuZr$
a, Å	16.640 (3)	13.386 (3)	13.031 (3)
b, Å	13.936 (3)	22.514 (6)	14.880 (4)
c, Å	13.290 (3)	10.639 (3)	15.594 (3)
β, deg		91.89 (2)	108.08 (2)
V, Å^3	3082 (2)	3205 (3)	2874 (2)
Z	4	4	4
molecular weight	684.35	698.39	656.30
space group	*Pnma*	$P2_1/c$	$P2_1/n$
no. of reflcns collected	7859	6042	8996
no. of unique reflns ($F_o > 0$)	3376	4386	6744
no. of reflcns used ($F_o > 3\sigma(F_o)$)	2527	3000	4658
$R_{averaging}$ ($F_o > 0$)	0.029		
ρ(calcd), g cm^{-3}	1.475	1.447	1.516
radiation	Mo Kα (graphite monochromatized)	Mo Kα (graphite monochromatized)	Mo Kα (graphite monochromatized)
μ, cm^{-1}	10.2	9.79	10.9
transmissn coeff: max, min	0.708, 0.637	0.895, 0.796	0.835, 0.596
R	0.049	0.064	0.062
R_W	0.058	0.066	0.080
max shift/error, final cycle	≤0.1	≤0.02	≤0.01
temp, K	200	200	200

both resonance structures, being singly bonded to one carbon and doubly bonded to the other.

The zwitterionic resonance form

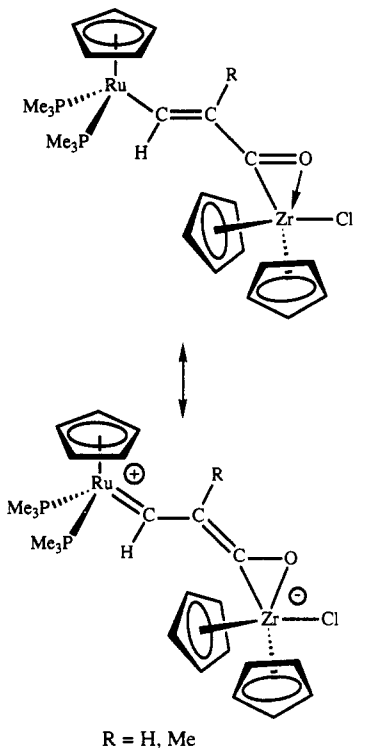

R = H, Me

for the η^2-iminoacyl complexes **2Ht**, **3H**, and **3Me** are analogous to those proposed[3a] in the η^2-acyl complexes resulting from reaction of CO with **1H** and **1Me**. In the case of these η^2-acyl products, spectroscopic data for $Cp(PMe_3)_2RuCH{=}CHC(O)ZrClCp_2$ and $Cp(PMe_3)_2RuCH{=}CMeC(O)ZrClCp_2$ were similar, indicating no substantial differences for R = H vs R = Me. The spectroscopic data, together with the structural data for $Cp(PMe_3)_2RuCH{=}CHC(O)ZrClCp_2$, were interpreted[3a] to be indicative of the zwitterionic resonance forms being more important than the neutral resonance form. We believe that the relative contribution of the zwitterionic resonance form (compared to the neutral resonance form) for the η^2-iminoacyl complexes **2Ht**, **3H**, and **3Me** is significant, though less than in the η^2-acyl analogues. Supporting this contention is the observation that the ^1H and ^{13}C NMR resonances of RuCH moiety in $Cp(PMe_3)_2RuCH{=}CHC(O)ZrClCp_2$ appear at δ 11.70 and 246.5, which are even more downfield than is found in **2Ht**.

Table IV. Bond Angles in 2Ht, 2Me, and 3Me

angle (deg)	2Ht	2Me	3Me
P(1)–Ru–P(2)	96.4 (1)	95.7 (1)	94.5 (1)
Ru–C(3)–C(2)	128.5 (6)	132.9 (9)	132.9 (6)
C(3)–C(2)–C(1)	121.3 (7)	120 (1)	118.5 (8)
C(2)–C(1)–N	133.4 (7)	138 (1)	134.6 (8)
C(1)–N–C(11)	129.1 (7)	134 (1)	135.5 (8)
Cl–Zr–C(1)	120.8 (2)	118.7 (2)	114.8 (2)
C(2)–C(1)–Zr	154.4 (7)	148.8 (8)	155.2 (6)
Cl–Zr–N	87.1 (2)	86.3 (2)	80.7 (2)
C(1)–N–Zr	74.1 (4)	75.0 (7)	75.7 (5)
N–C(1)–Zr	72.2 (4)	72.5 (7)	70.1 (5)
C(11)–N–Zr	156.7 (5)	150.9 (8)	148.9 (6)

Table V. Bond Distances in 2Ht, 2Me, and 3Me

distance (Å)	2Ht	2Me	3Me
Ru–C(3)	2.032 (7)	2.066 (10)	2.040 (8)
C(3)–C(2)	1.370 (10)	1.318 (14)	1.342 (11)
C(2)–C(1)	1.431 (10)	1.453 (14)	1.439 (11)
C(1)–N	1.276 (9)	1.243 (13)	1.293 (11)
Zr–C(1)	2.213 (8)	2.230 (11)	2.228 (8)
Zr–N	2.190 (6)	2.202 (10)	2.162 (8)
Zr–Cl	2.563 (2)	2.587 (4)	2.583 (2)
Ru–P(1)	2.255 (2)	2.252 (3)	2.249 (2)
Ru–P(2)	2.255 (2)	2.245 (3)	2.266 (2)

Structures of Three η^2-Iminoacyl Complexes Determined by X-ray Crystallography. The molecular structures of **2Ht**, **2Me**, and **3Me** were determined by single-crystal X-ray diffraction. Details of the data collection and refinement parameters are given in Table III, and additional crystallographic data are given in the supplementary material. ORTEP diagrams of **2Ht**, **2Me**, and **3Me** are shown in Figures 3–5, and bond angles and distances are given in Tables IV and V. Positional parameters for the non-hydrogen atoms are listed in Tables VI–VIII. In all three structures, the bond lengths and angles are virtually identical for the two metal fragments, $Cp(PMe_3)_2Ru$ and Cp_2ZrCl, but the relationship between these metal fragments and the bridging CHC(R)CN(R′)

Table VI. Atomic Coordinates[a] for the Non-Hydrogen Atoms in $Cp(PMe_3)_2RuCH{=}CHCNC(CH_3)_3ZrClCp_2$ (2Ht)

atom	x	y	z
Ru	0.48540 (3)	0.2500	0.34185 (4)
P(1)	0.39634 (8)	0.12938 (12)	0.36053 (10)
C(111)	0.3682 (6)	0.0991 (6)	0.4883 (5)
C(112)	0.4345 (6)	0.0182 (6)	0.3169 (7)
C(113)	0.2972 (5)	0.1296 (7)	0.3022 (8)
C(21)[b]	0.5630 (8)	0.2500	0.4860 (10)
C(22)[b]	0.5824 (7)	0.1614 (9)	0.4196 (9)
C(23)[b]	0.6142 (7)	0.1972 (9)	0.3273 (9)
C(21')[b]	0.6192 (10)	0.2500	0.3263 (12)
C(22')[b]	0.6024 (12)	0.1696 (15)	0.3661 (15)
C(23')[b]	0.5716 (8)	0.2013 (11)	0.4609 (10)
C(3)	0.4580 (4)	0.2500	0.1929 (5)
C(2)	0.5093 (5)	0.2500	0.1122 (6)
C(1)	0.4796 (4)	0.2500	0.0111 (6)
N	0.5137 (4)	0.2500	−0.0749 (5)
C(11)	0.6011 (5)	0.2500	−0.0996 (6)
C(12)	0.6101 (6)	0.2500	−0.2122 (7)
C(13)	0.6395 (4)	0.1621 (6)	−0.0567 (6)
Zr	0.38434 (4)	0.2500	−0.10503 (5)
Cl	0.42003 (17)	0.2500	−0.29261 (16)
C(31)	0.2968 (5)	0.1336 (6)	−0.0100 (6)
C(33)	0.3858 (6)	0.0675 (6)	−0.1151 (8)
C(34)	0.3173 (8)	0.0997 (8)	−0.1703 (6)
C(35)	0.2660 (5)	0.1376 (7)	−0.1027 (8)

[a] Numbers in parentheses are estimated standard deviations in the least significant digit(s). [b] Atoms C22, C23, C22', and C23' have site occupancy factors of 0.5. Atoms C21 and C21' have site occupancy factors of 0.25.

Table VII. Atomic Coordinates[a] for the Non-Hydrogen Atoms in $Cp(PMe_3)_2RuCH{=}C(CH_3)CNC(CH_3)_3ZrClCp_2$ (2Me)

atom	x	y	z
Ru	0.24308 (7)	0.10408 (5)	0.41389 (9)
P(1)	0.3722 (2)	0.14601 (15)	0.3164 (3)
C(111)	0.3613 (10)	0.1691 (6)	0.1516 (13)
C(112)	0.4832 (8)	0.0985 (6)	0.3130 (13)
C(113)	0.4260 (10)	0.2125 (6)	0.3863 (14)
P(2)	0.1249 (3)	0.16262 (17)	0.3247 (4)
C(221)	0.0018 (9)	0.1542 (7)	0.3927 (14)
C(222)	0.1404 (11)	0.2414 (7)	0.3374 (17)
C(223)	0.0851 (10)	0.1558 (7)	0.1625 (14)
C(21)	0.1640 (11)	0.0664 (8)	0.5773 (12)
C(22)	0.2029 (13)	0.1221 (7)	0.6125 (11)
C(23)	0.3053 (13)	0.1184 (9)	0.6094 (14)
C(24)	0.3288 (12)	0.0606 (9)	0.5707 (13)
C(25)	0.2422 (13)	0.0301 (7)	0.5523 (14)
C(3)	0.2341 (8)	0.0453 (5)	0.2648 (10)
C(2)	0.1757 (8)	−0.0005 (5)	0.2389 (10)
C(2')	0.0824 (8)	−0.0152 (6)	0.3104 (12)
C(1)	0.2131 (8)	−0.0497 (5)	0.1656 (11)
N	0.2401 (7)	−0.0586 (4)	0.0566 (9)
C(11)	0.2355 (10)	−0.0225 (6)	−0.0629 (12)
C(12)	0.1680 (10)	0.0310 (6)	−0.0540 (12)
C(13)	0.3413 (10)	−0.0033 (7)	−0.0878 (12)
C(14)	0.1966 (11)	−0.0624 (7)	−0.1669 (12)
Zr	0.28363 (8)	−0.13938 (5)	0.16116 (11)
Cl	0.3672 (3)	−0.17336 (16)	−0.0425 (4)
C(31)	0.1378 (9)	−0.1985 (6)	0.0633 (13)
C(32)	0.2019 (10)	−0.2394 (6)	0.1266 (15)
C(33)	0.2019 (11)	−0.2304 (7)	0.2500 (15)
C(34)	0.1404 (10)	−0.1834 (7)	0.2757 (14)
C(35)	0.0981 (9)	−0.1642 (6)	0.1602 (15)
C(41)	0.3782 (10)	−0.0811 (7)	0.3273 (14)
C(42)	0.4430 (9)	−0.0859 (6)	0.2318 (14)
C(43)	0.4685 (10)	−0.1440 (7)	0.2178 (15)
C(44)	0.4208 (11)	−0.1780 (6)	0.3090 (16)
C(45)	0.3652 (11)	−0.1377 (8)	0.3771 (13)

[a] Numbers in parentheses are estimated standard deviations in the least significant digit(s).

ligand varies within the three complexes. In **2Ht** there is a crystallographically imposed mirror plane that confines Ru, C(3), H(3), C(2), H(2), C(1), N, C(11), C(12), Zr, and Cl to the same plane. The two PMe_3 groups, the two Cp ligands on Zr, and two of the methyls of the ^{t}Bu group are all symmetrically located on either side of the mirror plane. No such mirror plane is present in **2Me**. Comparison of Figures 3 and 4 shows a notable difference in the structures

Scheme III

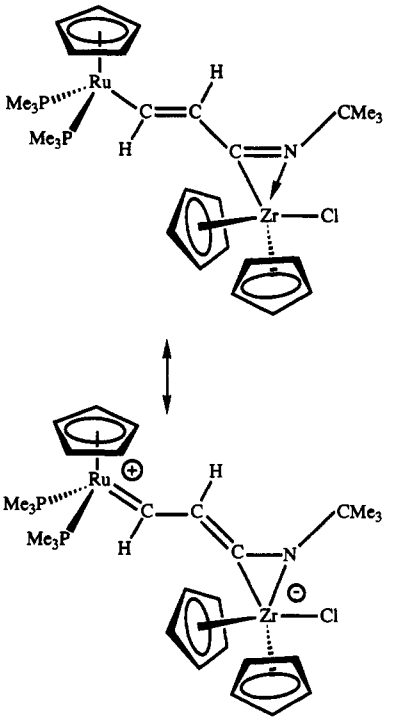

2Ht

Table VIII. Atomic Coordinates[a] for the Non-Hydrogen Atoms in $Cp(PMe_3)_2RuCH{=}C(CH_3)CNCH_3ZrClCp_2$ (3Me)

atom	x	y	z
Ru	0.10979 (5)	0.21570 (4)	0.74591 (4)
P(1)	0.06156 (19)	0.07624 (14)	0.69317 (15)
C(111)	−0.0701 (8)	0.0710 (7)	0.6015 (8)
C(112)	0.1476 (9)	0.0237 (7)	0.6392 (7)
C(113)	0.0414 (10)	−0.0138 (6)	0.7641 (7)
P(2)	0.21064 (17)	0.16877 (15)	0.88474 (15)
C(221)	0.1483 (8)	0.1200 (6)	0.9615 (6)
C(222)	0.3228 (8)	0.0897 (7)	0.8900 (8)
C(223)	0.2880 (7)	0.2557 (7)	0.9564 (6)
C(31)	0.1560 (10)	0.3608 (7)	0.7370 (8)
C(32)	0.0620 (9)	0.3416 (7)	0.6646 (9)
C(33)	0.0877 (9)	0.2781 (8)	0.6109 (7)
C(34)	0.2009 (8)	0.2559 (7)	0.6497 (7)
C(35)	0.2397 (8)	0.3071 (8)	0.7307 (7)
C(3)	−0.0247 (6)	0.2178 (5)	0.7865 (5)
C(2)	−0.0617 (7)	0.2764 (6)	0.8353 (6)
C(2')	0.0019 (7)	0.3549 (6)	0.8853 (7)
C(1)	−0.1687 (7)	0.2637 (5)	0.8414 (6)
N	−0.2279 (6)	0.3057 (5)	0.8813 (5)
C(11)	−0.2144 (8)	0.3843 (7)	0.9391 (7)
Zr	−0.32785 (6)	0.19527 (6)	0.81284 (6)
Cl	−0.46415 (17)	0.27600 (17)	0.87639 (16)
C(41)	−0.1930 (10)	0.0819 (9)	0.9001 (12)
C(42)	−0.2623 (17)	0.0366 (9)	0.8359 (9)
C(43)	−0.3598 (17)	0.0337 (11)	0.8459 (13)
C(44)	−0.3543 (12)	0.0801 (12)	0.9231 (13)
C(45)	−0.2520 (13)	0.1103 (8)	0.9610 (8)
C(51)	−0.3179 (9)	0.2313 (9)	0.6584 (6)
C(52)	−0.3939 (10)	0.2873 (8)	0.6686 (7)
C(53)	−0.4837 (9)	0.2429 (10)	0.6722 (8)
C(54)	−0.4593 (11)	0.1505 (9)	0.6634 (8)
C(55)	−0.3547 (11)	0.1468 (9)	0.6530 (7)

[a] Numbers in parentheses are estimated standard deviations in the least significant digit(s).

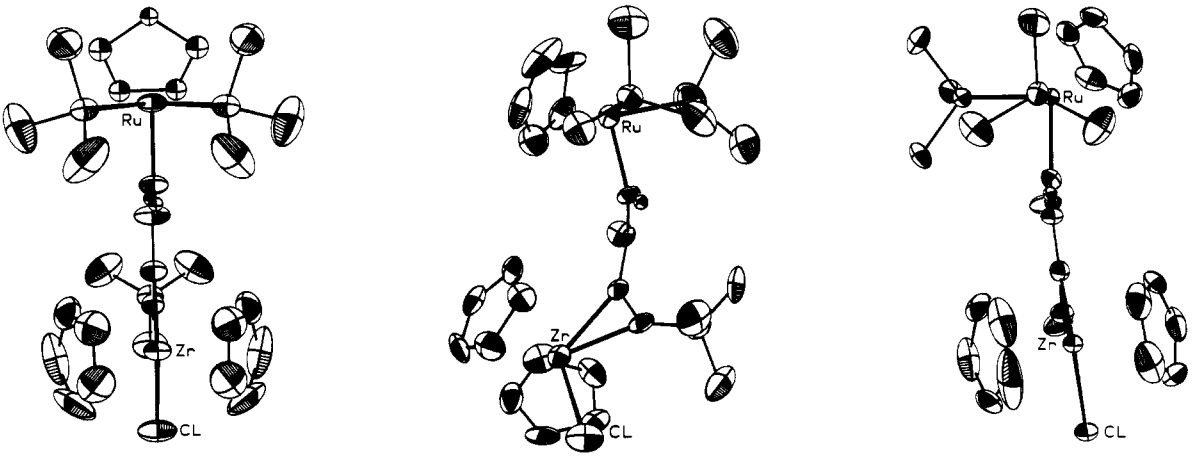

Figure 6. ORTEP drawings of the three η^2-iminoacyl compounds with the CHC(R) portions of the bridging ligand perpendicular to the plane of the paper: (a, left) **2Ht**; (b, center) **2Me**, (c, right) **3Me**.

Table IX. Dihedral Angles (deg) in 2Ht, 2Me, and 3Me

plane 1/plane 2	2Ht	2Me	3Me
Ru-C(3)-C(2)/P(1)-Ru-C(3)	-48.3	-1.4	6.8
Ru-C(3)-C(2)/P(2)-Ru-C(3)	48.3	94.2	101.9
P(1)-Ru-C(3)/P(2)-Ru-C(3)	96.5	95.6	95.1
Ru-C(3)-C(2)/C(2)-C(1)-Zr	0	70.8	9.0
C(1)-N-Zr/C(1)-Zr-Cl	0	5.9	4.6

of **2Ht** and **2Me** in terms of how the "Zr half" of the molecule is oriented compared to the "Ru half". This difference in **2Ht** and **2Me** is due to a rotation around the C(1)–C(2) bond. This rotation prevents the methyl group of **2Me** (C(2′)) from having a sterically unfavorable contact with the ^{t}Bu group of the iminoacyl ligand. The differences between **2Ht** and **2Me** are also evident in Figure 6, which displays ORTEP views of **2Ht**, **2Me**, and **3Me** with the CHC(R) portion of the bridging ligand perpendicular to the plane of the paper. Dihedral angles are given in Table IX. Because of the rotation about the C(1)–C(2) bond, the dihedral angle between the Ru–C(3)–C(2) plane and the C(2)–C(1)–Zr plane is 70.8° in **2Me**, whereas it is 0° in **2Ht** due to the crystallographic mirror plane.

The smaller isocyanide in **3Me** allows it to adopt a conformation similar to that of **2Ht**. As can be seen in Figure 6, the CHCMeCNMe ligand of **3Me** is nearly planar, with the dihedral angle being only 9°. The largest deviation of the non-hydrogen atoms of the bridging ligand and the Zr from the least-squares best plane containing these atoms is ±0.004 Å. The Ru atom, which was not included in this plane, lies 0.221 Å out of the plane.

The Zr portion and the bridging ligand have similar structures in **2Ht** and **3Me**, but the orientation of the $Cp(PMe_3)_2Ru$ fragment to the rest of the molecule is different for these two complexes. While the two PMe_3 ligands are symmetrically located on opposite sides of the mirror plane in **2Ht**, the $Cp(PMe_3)_2Ru$ fragment is rotated in both **2Me** and **3Me** such that one P is almost coplanar with the Ru–C(3)–C(2) plane and the other P is nearly perpendicular to it (see Figure 6 and the dihedral angles in Table IX). Thus, the $Cp(PMe_3)_2Ru$ part of **3Me** is similar to that in **2Me**, while the orientation of the bridging ligand and Cp_2ZrCl portions of **3Me** resemble those of **2Ht**.

Despite these differences in *dihedral angles*, the *bond angles* are similar in **2Ht** and **2Me** (Table IV). Especially revealing is the trend in comparative bond *distances* (Table V) for the bonds which are single bonds in one resonance form and double bonds in the other. Both the Ru–C(3) distance and the C(2)–C(1) distance are shorter in **2Ht** compared to **2Me**, whereas the opposite is true for the C(3)–C(2) distance and the C(1)–N distances. Although the differences in distances are not large when the experimental uncertainties are taken into account, we believe that this trend accurately reflects the difference in electronic structures of the two related compounds. Furthermore, these structural data lead to the same conclusion as that reached from the evaluation of the spectroscopic data—that the contribution of the zwitterionic resonance form is much more important for **2Ht** than for **2Me**.

The results discussed above provide an explanation of how the presence or absence of a methyl group on C(2) is able to exert such a strong influence on the spectroscopic and structural properties of the η^2-iminoacyl complexes. The disparate electronic properties of the ruthenium and zirconium moieties are integral features that facilitate the intramolecular charge transfer which leads to the zwitterionic resonance form. The electron-rich ruthenium, with two PMe_3 ligands, helps to stabilize the formal positive charge on the Ru=C carbene portion of the zwitterionic resonance form. Along with the difference in electronic nature of the two metals, however, an additional requirement for the viability of the zwitterionic resonance form appears to be the ability of the organic bridging unit to achieve coplanarity with the two metals. This is rigorously attained in **2Ht**, where a mirror plane exists, but is effectively precluded in **2Me** due to the presence of the methyl group. If the hydrogen on C(2) in **2Ht** were replaced by a methyl group and the conformation maintained, then this methyl group would have an unfavorable steric contact with the nearby ^{t}Bu group. The calculated distances between this carbon and the two closest carbons of the ^{t}Bu group in this model are 2.8 and 3.0 Å. This hypothetical conformation is avoided, since, as shown by the crystallographic data, the actual structure of **2Me** is one in which the methyl group and ^{t}Bu group are oriented far apart, by rotation around the C(1)–C(2) bond. In **2Me**, the distance between C(2′) and the closest carbon of the ^{t}Bu group is 4.2 Å, which is similar to the *inter*molecular methyl–methyl distances.

Spectroscopic data for both **3H** and **3Me** are similar to those of **2Ht** (Table II), indicating that they both have a viable zwitterionic resonance form. The methyl group in **3Me** has only a minor effect on spectroscopic properties compared to **3H**, as opposed to the dramatic differences in spectra and structure for **2Ht** vs **2Me**. It is clear that large changes *can* be caused by a single methyl group in these compounds, but only when it is present in conjunction with a bulky group (^{t}Bu) on the iminoacyl ligand.

The severe steric congestion that would result in **2Me** is avoided, since **2Me** adopts a different structure than its nonmethylated analogue **2Ht**.

Conclusions and Summary

The reaction of $Cp(PMe_3)_2RuCH{=}CHZrClCp_2$ with ^{t}BuNC initially gives a kinetic isomer of an η^2-iminoacyl complex which cleanly rearranges to the thermodynamic isomer; the activation parameters for this rearrangement were determined. The reaction with ^{t}BuNC is over 100 times faster for the dimetalloethylene complex $Cp(PMe_3)_2RuCH{=}CHZrClCp_2$ compared to the dimetallopropylene complex $Cp(PMe_3)_2RuCH{=}C(CH_3)ZrClCp_2$. Evaluation of the spectroscopic and structural data for the two η^2-iminoacyl complexes leads to the conclusion that the electronic structure of $Cp(PMe_3)_2RuCH{=}CHC(N^tBu)ZrClCp_2$ has a considerable contribution from a zwitterionic resonance form, while the closely related methyl derivative $Cp(PMe_3)_2RuCH{=}CMeC(N^tBu)ZrClCp_2$ does not. Steric inhibition of resonance in the methyl derivative is suggested to cause these differences, due to an unfavorable interaction of the methyl group and the ^{t}Bu group in a conformation that would have allowed coplanarity of all of the atoms in the bridging ligand between the two metals. This coplanarity is rigorously attained in $Cp(PMe_3)_2RuCH{=}CHC(N^tBu)ZrClCp_2$, where a crystallographically imposed mirror plane constrains the two metals and the bridging ligand to reside in the same plane. Spectroscopic and structural studies of the η^2-iminoacyl derivatives prepared from the less sterically demanding isocyanide MeNC are consistent with a contribution from the zwitterionic resonance form for both $Cp(PMe_3)_2RuCH{=}CHC(NMe)ZrClCp_2$ and $Cp(PMe_3)_2RuCH{=}CMeC(NMe)ZrClCp_2$.

Experimental Section

General Procedures. All manipulations of oxygen- or water-sensitive compounds were carried out under an atmosphere of argon using Schlenk or vacuum-line techniques or in a Vacuum Atmospheres drybox. Glassware was dried in a 120 °C oven for several hours, or was flame-dried and cooled under vacuum prior to use. ^{1}H (300-MHz) and ^{13}C NMR (75-MHz) spectra were recorded on a Bruker AM-300 spectrometer. ^{13}C NMR spectra were recorded in the presence of $Cr(acac)_3$ (0.04–0.07 M). The ^{1}H chemical shifts were referenced to the residual proton peak of the solvent: C_6D_5H, δ 7.15; $CHDCl_2$, δ 5.32; CHD_2CN, δ 1.93. The ^{13}C chemical shifts were referenced to the central peak of CD_2Cl_2 (δ 53.8) or the CD_3 of $C_6D_5CD_3$ (δ 20.4). $^1J_{CH}$ coupling constants were obtained from ^{13}C NMR spectra using gated decoupling. The PMe_3 resonances in these compounds do not appear as a simple first-order pattern in the NMR. In the ^{1}H NMR, the PMe_3 resonances appear as a $A_9XX'A'_9$ pattern; the appearance of these resonances in the ^{1}H NMR is a "filled-in doublet", with the separation of the outer lines being equal to $^2J_{PH} + {}^4J_{PH}$.[9] In the $^{13}C\{^1H\}$ NMR, the PMe_3 resonance appears as a virtual triplet (designated as vt in the spectral assignments below); the observed coupling constant J is equal to $^1J_{PC} + {}^3J_{PC}$.[9] IR spectra were recorded on a Mattson Polaris FT-IR. Elemental analyses were carried out by Schwarzkopf Microanalytical Laboratory or by Galbraith Laboratory.

Materials. THF was distilled from Na/benzophenone. Hexane was stirred over concentrated H_2SO_4 until the H_2SO_4 remained colorless and was then distilled from Na/benzophenone and stored over $[Cp_2TiCl]_2ZnCl_2$.[10] Diethyl ether was stored over $[Cp_2TiCl]_2ZnCl_2$ and vacuum transferred immediately prior to use. Benzene-d_6 was dried over NaK and stored over $[Cp_2TiCl]_2ZnCl_2$. Dichloromethane-d_2 was dried over P_2O_5 and stored over CaH_2. *tert*-Butyl isocyanide (Aldrich) and methyl isocyanide (Quantum Design Inc., Austin, TX) were stored over activated 3-Å molecular seives and manipulated on a high-vacuum line using calibrated gas bulbs. $Cp(PMe_3)_2RuCH{=}CRZrClCp_2$ (R = H, **1H**; R = Me, **1Me**) were prepared as previously described.[3]

$Cp(PMe_3)_2RuCH{=}CHC(N^tBu)ZrClCp_2$ (2Ht). Complex **1H** (178 mg, 0.30 mmol) was dissolved in neat ^{t}BuNC (~5 mL) to give an orange solution which formed a yellow precipitate in ~0.5 h. The excess ^{t}BuNC was recovered by vacuum transfer, and the yellow residue was dissolved in THF and filtered. The THF filtrate was concentrated to the point of precipitation, and Et_2O was added to complete the precipitation. The product was isolated by filtration, washed with Et_2O, and dried under vacuum to give a bright yellow solid (158 mg, 78% yield, >98% purity by ^{1}H NMR). Analytically pure crystals were obtained from vapor diffusion of Et_2O into a THF solution of **2Ht**. ^{1}H NMR (CD_2Cl_2): δ 10.02 (dt, $^3J_{HH}$ = 16 Hz, $^3J_{PH}$ = 8 Hz, 1 H, RuCH), 7.71 (dt, $^3J_{HH}$ = 16 Hz, $^4J_{PH}$ = 1 Hz, 1 H, RuC=CH), 5.75 (s, 10 H, CpZr), 4.76 (s, 5 H, RuCp), 1.47 (filled-in doublet, $^2J_{PH} + {}^4J_{PH}$ = 9 Hz, 18 H, PMe_3), 1.35 (s, 9 H, CMe_3). ^{13}C NMR (CD_2Cl_2, 0.05 M $Cr(acac)_3$): δ 216.5 (d, $^2J_{CH}$ = 8 Hz, C=N), 214.2 (dt, $^1J_{CH}$ = 127 Hz, $^2J_{PC}$ = 17 Hz, RuC), 136.4 (dt, $^1J_{CH}$ = 152 Hz, $^3J_{PC}$ = 3 Hz, RuC=*C*), 108.2 (d, $^1J_{CH}$ = 172 Hz, CpZr), 83.6 (d, $^1J_{CH}$ = 174 Hz, CpRu), 60.7 (s, *C*Me_3), 30.2 (q, $^1J_{CH}$ = 127 Hz, C*Me*$_3$), 23.1 (q of vt, $^1J_{CH}$ = 131 Hz, $^1J_{PC} + {}^3J_{PC}$ = 29 Hz, PMe_3). IR (KBr): ν(C=N) 1547 cm^{-1}, ν(C=C) 1459 cm^{-1}. Anal. Calcd for $C_{28}H_{44}ClNP_2RuZr$: C, 49.13; H, 6.49; N, 2.05. Found: C, 49.20; H, 6.36; N, 1.98.

$Cp(PMe_3)_2RuCH{=}CMeC(N^tBu)ZrClCp_2$ (2Me). Complex **1Me** (259 mg, 0.42 mmol) was dissolved in neat ^{t}BuNC (~5 mL) and worked up as described for **2Ht** to give a bright yellow solid (173 mg, 59% yield, ~90% purity by ^{1}H NMR). A second crop from THF/hexanes was also obtained (35 mg of yellow solid, 12% yield, ~75% purity by ^{1}H NMR). Analytically pure crystals were obtained from vapor diffusion of Et_2O into a THF solution of **2Me**. ^{1}H NMR (CD_2Cl_2): δ 6.87 (tq, $^3J_{PH}$ = 10 Hz, $^4J_{HH}$ = 1 Hz, 1 H, RuCH), 5.77 (s, 10 H, CpZr), 4.61 (s, 5 H, RuCp), 2.09 (br s, 3 H, C=CMe), 1.42 (filled-in doublet, $^2J_{PH} + {}^4J_{PH}$ = 8 Hz, 18 H, PMe_3), 1.33 (s, 9 H, CMe_3). ^{13}C NMR (CD_2Cl_2, 0.06 M $Cr(acac)_3$): δ 227.7 (s, C=N), 153.4 (dt, $^1J_{CH}$ = 123 Hz, $^2J_{PC}$ = 17 Hz, RuC), 141.0 (t, $^3J_{PC}$ = 4 Hz, RuC=*C*), 108.9 (d, $^1J_{CH}$ = 172 Hz, CpZr), 80.9 (d, $^1J_{CH}$ = 173 Hz, CpRu), 61.0 (s, *C*Me_3), 29.0 (q, $^1J_{CH}$ = 128 Hz, C*Me*$_3$), 24.1 (q, $^1J_{CH}$ = 127 Hz, C=C*Me*), 23.3 (q of vt, $^1J_{CH}$ = 126 Hz, $^1J_{PC} + {}^3J_{PC}$ = 29 Hz, PMe_3). IR (KBr): ν(C=N) 1626 cm^{-1}, ν(C=C) 1498 cm^{-1}. Anal. Calcd for $C_{29}H_{46}ClNP_2RuZr$: C, 49.87; H, 6.65; N, 2.01. Found: C, 49.85; H, 6.21; N, 2.23.

$Cp(PMe_3)_2RuCH{=}CHC(NMe)ZrClCp_2$ (3H). Complex **1** (182 mg, 0.30 mmol) was dissolved in neat MeNC (~ 2 mL) and worked up as described for **2Ht** to give a yellow solid (152 mg, 78% yield, >95% purity by ^{1}H NMR). A second crop from THF/hexanes yielded 19 mg (10% yield, 89% purity by ^{1}H NMR). Analytically pure crystals were obtained from vapor diffusion of Et_2O into a THF solution of **3H**. ^{1}H NMR (CD_2Cl_2): δ 10.09 (dt, $^3J_{HH}$ = 16 Hz, $^3J_{PH}$ = 9 Hz, 1 H, RuCH), 7.42 (dt, $^3J_{HH}$ = 16 Hz, $^4J_{PH}$ = 1 Hz, 1 H, RuC=CH), 5.75 (s, 10 H, CpZr), 4.79 (s, 5 H, RuCp), 2.94 (s, 3 H, Me), 1.48 (filled-in doublet, $^2J_{PH} + {}^4J_{PH}$ = 9 Hz, 18 H, PMe_3). ^{13}C NMR (CD_2Cl_2, 0.07 M $Cr(acac)_3$): δ 218.3 (s, C=N), 216.6 (dt, $^1J_{CH}$ = 127 Hz, $^2J_{PC}$ = 17 Hz, RuC), 134.8 (dt, $^1J_{CH}$ = 150 Hz, $^3J_{PC}$ = 3 Hz, RuC=*C*), 107.9 (d, $^1J_{CH}$ = 172 Hz, CpZr), 83.6 (d, $^1J_{CH}$ = 174 Hz, CpRu), 32.3 (q, $^1J_{CH}$ = 136 Hz, CN*Me*), 22.7 (q of vt, $^1J_{CH}$ = 127 Hz, $^1J_{PC} + {}^3J_{PC}$ = 29 Hz, PMe_3). IR (KBr): ν(C=N) 1576 cm^{-1}, ν(C=C) 1462 cm^{-1}. Anal. Calcd for $C_{25}H_{38}ClNP_2RuZr$: C, 46.75; H, 5.98; N, 2.18. Found: C, 46.71; H, 6.02; N, 2.19.

$Cp(PMe_3)_2RuCH{=}CMeC(NMe)ZrClCp_2$ (3Me). Complex **1Me** (132 mg, 0.21 mmol) was dissolved in neat MeNC (~2 mL) and worked up as described for **2Ht** to give a yellow solid (86 mg, 62% yield, ~77% purity by ^{1}H NMR). A second crop from THF/hexanes yielded 13 mg (9% yield, >90% purity by ^{1}H NMR). Analytically pure crystals were obtained from vapor diffusion of Et_2O into a THF solution of **3Me**. ^{1}H NMR (CD_2Cl_2): δ 9.59 (t, $^3J_{PH}$ = 11 Hz, 1 H, RuCH), 5.73 (s, 10 H, CpZr), 4.71 (s, 5 H, CpRu), 3.24 (s, 3 H, CNMe), 2.23 (s, 3 H, RuC=CMe), 1.48 (filled-in doublet, $^2J_{PH} + {}^4J_{PH}$ = 8 Hz, 18 H, PMe_3). ^{13}C NMR (CD_2Cl_2, 0.07 M $Cr(acac)_3$): δ 219.4 (s, CN), 208.7 (dt, $^1J_{CH}$ = 129 Hz, $^2J_{PC}$ = 17 Hz, RuC), 142.8 (s, RuC=*C*), 107.8 (d, $^1J_{CH}$ = 172 Hz, CpZr), 81.5 (d, $^1J_{CH}$ = 174 Hz, CpRu), 33.8 (q, $^1J_{CH}$ = 137 Hz, CM*Me*), 22.8 (q of vt, $^1J_{CH}$ = 122 Hz, $^1J_{PC} + {}^3J_{PC}$ = 29 Hz,

(9) (a) Redfield, D. A.; Cary, L. W.; Nelson, J. H. *Inorg. Chem.* **1975**, *14*, 50–59. (b) Redfield, D. A.; Nelson, J. H.; Cary, L. W. *Inorg. Nucl. Chem. Lett.* **1974**, *10*, 727–733.

(10) Sekutowski, D. G.; Stucky, G. D. *Inorg. Chem.* **1975**, *9*, 2192–2199.

PMe_3), 21.9 (q, $^1J_{CH}$ = 114 Hz, RuC=C*Me*). IR (KBr): ν(C=N) 1595 cm^{-1}, ν(C=C) 1465 cm^{-1}. Anal. Calcd for $C_{26}H_{40}ClNP_2RuZr$: C, 47.58; H, 6.16; N, 2.13. Found: C, 47.56; H, 6.32; N, 2.22.

Formation and Spectroscopic Characterization of 2Hk. A 5-mm NMR tube was charged with **1H** (15.8 mg, 0.026 mmol), ^{t}BuNC (0.026 mmol, measured with a calibrated gas bulb), 1,4-bis(trimethylsilyl)benzene (1.2 mg, internal standard), and CD_2Cl_2 (0.54 mL) and stored at −78 °C prior to insertion into the NMR probe. Little reaction was observed after 1 h at 200 K, and only ~15% conversion to **2Hk** was observed after 30 min at 240 K. The solution was warmed to 260 K and maintained at that temperature for 3.5 h, during which time **2Hk** became the predominant species (>70%), with small amounts (~15%) of the thermodynamic isomer **2Ht** and a trace of starting material **1H** still present. ^{1}H NMR (CD_2Cl_2) of **2Hk**: δ 10.49 (dt, $^3J_{HH}$ = 15 Hz, $^3J_{PH}$ = 10 Hz, 1 H, RuCH), 7.66 (br d, $^1J_{HH}$ = 15 Hz, 1 H, RuC=CH), 5.86 (s, 10 H, CpZr), 4.71 (s, 5 H, CpRu), 1.40 (s, CMe_3), ~1.41 (PMe_3 resonance partially obscured by the CMe_3 resonance). The sample for ^{13}C NMR was similarly prepared in a 5-mm NMR tube and stored at −78 °C for 2 h before insertion into the probe. The sample was equilibrated at 260 K in the probe for 0.5 h prior to start of data acquisition. ^{13}C NMR resonances for both **2Hk** and **2Ht** were observed. $^{13}C\{^1H\}$ NMR of **2Hk** (CD_2Cl_2, 0.05 M Cr(acac)$_3$, 260 K): δ 222.1 (t, $^2J_{PC}$ = 16 Hz, RuC), 204.3 (s, C=N), 137.2 (s, RuC=*C*), 109.3 (s, CpZr), 83.0 (s, CpRu), 58.1 (s, *C*Me$_3$), 29.2 (s, C*Me*$_3$), 22.4 (vt, $^1J_{PC} + {}^3J_{PC}$ = 29 Hz, PMe_3).

Kinetics of Isomerization of 2Hk. A 5-mm NMR tube was charged with **1H** (11–15 mg), ^{t}BuNC (1.1 equiv), 1,4-bis(trimethylsilyl)benzene (~3 mg, internal standard), and CD_2Cl_2 (~0.5 mL). Samples were stored at 240 K for 7–30 h to form the kinetic isomer **2Hk** with very little formation of the thermodynamic isomer **2Ht**. The kinetics of disappearance of **2Hk** were then monitored by ^{1}H NMR at 254, 266, 281, and 296 K. The variable-temperature unit was calibrated[11] with MeOH (0.1% HCl). Peak heights of the CpZr and CpRu resonances (normalized to the internal standard) were recorded as a function of time. First-order kinetic treatment of the data, ln (peak height) vs time, gave k_{obs} at each temperature. Activation parameters were obtained from a plot of ln (k/T) vs $1/T$. Figure 1 shows only the first six data points collected at 254 K; the reaction was followed for 22 h, to 40% isomerization, and exhibited a linear first-order plot over this entire range.

Competition of Isocyanides for 1H and 1Me. A 5-mm NMR tube was charged with **1H** (4.3 mg, 0.007 mmol), **1Me** (18.5 mg, 0.030 mmol), 1,4-bis(trimethylsilyl)benzene (1.8 mg, internal standard), and CD_2Cl_2 (0.6 mL). The **1Me** to **1H** ratio was determined by ^{1}H NMR to be 4.66:1. ^{t}BuNC (0.005 mmol) was measured with a calibrated gas bulb and added by vacuum transfer. The insertion reaction was complete in ~2 h. The RuCp peak heights for **2Ht** and **2Me** were in a ratio of 27:1, indicating a kinetic preference of 127:1 for the insertion of ^{t}BuNC into **1H** over **1Me**. A similar competition experiment using MeNC indicated a preference of 116:1 for the insertion of MeNC into **1H** over **1Me**. Experiments in C_6D_6 gave results similar to those reported here in CD_2Cl_2.

Comparison of Rates of Reaction of MeNC for 1H and 1Me in Separate Tubes. To an NMR tube containing **1H** (~5 mg) in CD_2Cl_2 (0.5 mL) was added MeNC (1 equiv) via vacuum transfer. The reaction was ~50% complete in ~5 min and ~88% complete after 30 min as determined by ^{1}H NMR. Under similar conditions, the reaction of **1Me** (~5 mg) in CD_2Cl_2 (~0.5 mL) with MeNC (1 equiv) was ~10% complete after 4.5 h, ~73% complete after 4 days, and ~86% complete after 7 days as indicated by ^{1}H NMR.

Comparison of Rates of Reaction of ^{t}BuNC for 1H and 1Me in Separate Tubes. ^{t}BuNC (1 equiv) was added to a NMR tube containing **1H** (~6 mg) and C_6D_6 (0.5 mL). The insertion reaction was ~90% complete in 10 min, yielding about a 1:1 mixture of **2Hk** and **2Ht**. After 1.5 h, only **2Ht** was observed by ^{1}H NMR. Under similar conditions, addition of ^{t}BuNC (1 equiv) to a solution of **1Me** (~6 mg) in C_6D_6 (0.5 mL) was ~45% complete after 42 h, ~72% complete after 6 days, and ~90% complete after 13 days.

(11) Van Geet, A. L. *Anal. Chem.* **1970**, *42*, 679–680.

Collection and Reduction of X-ray Data. Crystals of **2Ht**, **2Me**, and **3Me** suitable for X-ray diffraction analysis were grown by vapor diffusion of Et_2O into THF at room temperature in a drybox. For each complex the crystal was coated with petroleum jelly and then mounted in a glass capillary. The crystals were initially studied with X-rays at room temperature to determine the crystal quality and crystal system. The crystals were then cooled to 200 K for collection of intensity data.

2Ht crystallizes as yellow prisms. A yellow crystal of dimensions 0.44 × 0.44 × 0.44 mm was used for the X-ray study. The diffraction data indicated orthorhombic symmetry with systematic absences $h0l$, $h + l = 2n + 1$, and $hk0$, $k = 2n + 1$, consistent with space groups $P2_1nb$ and $Pmnb$ (nonstandard settings of $Pna2_1$[12a] and $Pnma$,[12b] respectively). Solution and refinement of the structure indicated the centrosymmetric space group as the correct choice so the crystal parameters and intensity data were transformed to the standard setting, $Pnma$, and all data reported here for **2Ht** refer to this space group unless otherwise noted.

2Me crystallizes as yellow prisms. A crystal of dimensions 0.12 × 0.22 × 0.42 mm was used for the X-ray investigation. The diffraction data indicated monoclinic symmetry with systematic absences $h0l$, $h = 2n + 1$, and $0k0$, $h = 2n + 1$, consistent with space group $P2_1/a$ (a nonstandard setting of $P2_1/c$[12c]). The crystal parameters and intensity data were transformed to the standard setting, $P2_1/c$, which was used for the structure solution and refinement, and all data reported here refer to this space group unless otherwise noted.

3Me crystallizes as yellow prisms. A crystal of dimensions 0.20 × 0.35 × 0.45 mm was used for data collection. The diffraction data indicated monoclinic symmetry with systematic absences $h0l$, $h + l = 2n + 1$, and $0k0$, $k = 2n + 1$, consistent with space group $P2_1/n$ (a nonstandard setting of $P2_1/c$[12c]). All data reported here for **3Me** refer to the space group $P2_1/n$.

Crystal data are given in Table III, and additional details of the data collection and reduction are provided in Table S1 of the supplementary material.

Determination and Refinement of the Structures. **2Ht** and **2Me** were solved by standard Patterson[13] methods. **3Me** was solved using direct methods.[13] Difference Fourier maps were used to locate the remaining non-hydrogen atoms. The hydrogen atoms were placed at calculated positions (C–H = 0.95 Å) and allowed[13] to "ride" on the atom to which they were attached (hydrogens on the disordered cyclopentadienyl ligands of **2Ht** were not included in the refinement). A common isotropic thermal parameter was refined for all the hydrogen atoms in each structure. The quantity $\sum_w(|F_o| - |F_c|)^2$ was minimized during the least-squares refinement using absorption corrected data and neutral atom scattering factors[12d] and corrections for the effects of anomalous dispersion.[12e] Anisotropic thermal parameters were used for all the non-hydrogen atoms except for the disordered cyclopentadienyl ligands of **2Ht**. Additional crystallographic information is provided in the supplementary material.

Acknowledgment. This research was carried out at Brookhaven National Laboratory under Contract DE-AC02-76CH0016 with the U.S. Department of Energy and supported by its Division of Chemical Sciences, Office of Basic Energy Sciences. We thank Drs. Mark Andrews and George Gould for helpful discussions and an anonymous reviewer for helpful suggestions.

Supplementary Material Available: Additional experimental details of the X-ray diffraction structures (Table S1), complete listings of interatomic distances and angles (Tables S2–S4), final thermal parameters for the non-hydrogen atoms (Tables S5, S8, and S11), and calculated hydrogen atom positions (Tables S6, S9, and S12) (21 pages); listings of observed and calculated structure factors (Tables S7, S10, and S13) (44 pages). Ordering information is given on any current masthead page.

(12) *International Tables for X-Ray Crystallography*, 3rd ed.; Kynoch Press: Birmingham, England, 1969; (a) Vol. I, p 119; (b) Vol. I, p 151; (c) Vol. I, p 99; (d) Vol. IV, pp 99–101. (e) Anomalous dispersion effects were taken from: Cromer, D. T.; Liberman, D. *J. Chem. Phys.* **1970**, *53*, 1891–1898.

(13) Sheldrick, G. M. SHELX76, Crystal Structure refinement program, Cambridge University, England, 1976.